

IV. DISCUSSION

The rapidly converging moment solution recently used to determine the equivalent circuit parameters for an inductive post obstacle in a rectangular guide [1] has been extended to treat the post surface induced currents. It was found that the multifilamentary representation of the equivalent current can provide an accurate knowledge of the actual induced current. The procedure would presumably prove useful in resolving the induced current for other waveguide obstacles such as thick irises and posts of arbitrary shape that require, in general, more than just a few Fourier terms for their current representation.

A point should be made concerning the choice of the number of filaments N . The results presented in Section III exhibit a remarkable agreement with the exact solution with a number of sources as small as 10 per one-wavelength circumference. Note that, for any engineering needs, even a smaller number of sources could suffice.

The question of appropriately choosing the circular surface S_s has been dealt with, though indirectly, in the preceding section. The studies have shown that, with a fixed number of equivalent sources, the agreement with the exact solution is excellent within the range $0.1 \leq R_s/R_0 \leq 0.6$, where the value of the parameter R_s/R_0 is virtually of no importance. However, the results do deteriorate when the equivalent sources surface S_s approaches the post surface. This behavior has been already observed in connection with a numerical solution of two-dimensional electromagnetic wave diffraction [5]. Note that this is in contrast to the equivalent network parameters that are virtually independent of the choice of S_s [1]. This cardinal difference is attributable to the stationary character of the formula for the elements of this two-port network, which renders their calculation insensitive to small variations of the current about the true current.

REFERENCES

- [1] Y. Levitan, P. G. Li, A. T. Adams, and J. Perini, "Single-post inductive obstacle in rectangular waveguide," *IEEE Trans. Microwave Theory Tech.*, vol. MTT-31, pp. 806-812, Oct. 1983.
- [2] *Waveguide Handbook*, N. Marcuvitz, Ed., M.I.T. Rad. Lab. Ser., vol. 10. New York: McGraw-Hill, 1951, pp. 257-262.
- [3] P. G. Li, A. T. Adams, Y. Levitan, and J. Perini, "Multiple-post inductive obstacles in rectangular waveguides," *IEEE Trans. Microwave Theory Tech.*, vol. MTT-32, pp. 365-373, Apr. 1984.
- [4] Y. Levitan, P. G. Li, A. T. Adams, and J. Perini, "Single-post inductive obstacle in rectangular waveguide," Dept. Elec. Comput. Eng., Syracuse University, Tech. Rep. TR-82-13, Nov. 1982.
- [5] R. S. Popovici and Z. S. Tsvetkazashvili, "Numerical study of a diffraction problem by a modified method of non-orthogonal series," *U.S.S.R. Comput. Math. Phys.*, vol. 17, no. 2, pp. 93-103, 1977.

Modes in Anisotropic Rectangular Waveguides: An Accurate and Simple Perturbation Approach

ARUN KUMAR, M. R. SHENOY, AND K. THYAGARAJAN

Abstract—We present a simple and accurate perturbation method for obtaining the propagation characteristics of anisotropic rectangular waveguides described by a diagonal dielectric constant tensor. Comparison with the results of finite-element technique shows an excellent agreement.

Manuscript received January 4, 1984; revised April 24, 1984. This work was supported in part by the Department of Science and Technology, India. One of the authors (MRS) wishes to thank the Indian Institute of Technology, Delhi, for financial support.

The authors are with the Physics Department of the Indian Institute of Technology, New Delhi—110 016, India.

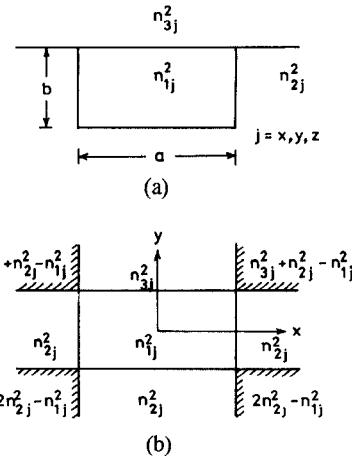


Fig. 1. (a) An embedded anisotropic channel waveguide with diagonal dielectric permittivity tensor. (b) The unperturbed structure used as a basis for obtaining the propagation characteristics of the waveguide shown in (a).

I. INTRODUCTION

The basic structural element common to many of the integrated optic devices is a single-mode channel waveguide. For an efficient design of devices, such as directional couplers, filters, and modulators, that are generally fabricated on an anisotropic substrate like LiNbO_3 [1], it is important to study the modal properties of anisotropic channel waveguides—the simplest of these consists of a homogeneous rectangular core. Achieving exact analytical solutions of such waveguides presents considerable difficulty, even for the isotropic case, due to the presence of corners. Numerical methods like the finite-element technique have been used for studying such problems [2]–[4]; however, these involve extensive and time-consuming computer calculations. Some approximate analytical techniques have also been presented [5], [6]; the effective index method [6] which can also be used for homogeneous core waveguides, has been shown to sometimes give ambiguous results [7]. The technique presented in [5] involves solving coupled transcendental equations, and also neglects the effect of corners, which, as we will show, becomes important near cutoff and for near-square cross section core waveguides.

In this paper, we present a simple and accurate method to obtain the propagation constants and the modal fields in homogeneous anisotropic channel waveguides described by a diagonal dielectric constant tensor. The results are compared with the finite-element method, and it is shown that our method gives highly accurate results, particularly for the fundamental modes.

II. METHOD

We consider a homogeneous anisotropic channel waveguide with each region characterized by a diagonal dielectric constant tensor. The principal dielectric constants of the core are denoted by n_{1x}^2 , n_{1y}^2 , n_{1z}^2 , and the substrate by n_{2x}^2 , n_{2y}^2 , n_{2z}^2 (see Fig. 1). In each region, the electric field satisfies the following equation:

$$\nabla(\nabla \cdot \mathbf{E}) - \nabla^2 \mathbf{E} = k_o \hat{k} \mathbf{E} \quad (1)$$

where k_o is the free-space wavenumber and \hat{k} represents the dielectric constant tensor.

The modes in channel waveguides can be classified into E_{pq}^y (polarized predominantly along the y -direction) and E_{pq}^x (polarized predominantly along the x -direction) modes [4], [6],

[8]. For E_{pq}^y modes, since E_x is very small, the y -component of (1) can be approximated by

$$\frac{\partial^2 E_y}{\partial x^2} + \frac{n_y^2}{n_z^2} \frac{\partial^2 E_y}{\partial y^2} + (k_o^2 n_y^2 - \beta_y^2) E_y = 0 \quad (2)$$

where we have used

$$\nabla \cdot \mathbf{D} = \epsilon_o n_y^2 \frac{\partial E_y}{\partial y} + \epsilon_o n_z^2 \frac{\partial E_z}{\partial z} = 0 \quad (3)$$

and a z -dependence of the field to be of the form $\exp(-i\beta_y z)$ is assumed, β_y representing the propagation constant of the E_{pq}^y mode.

Similarly, for the E_{pq}^x modes, E_x satisfies the following equation:

$$\frac{\partial^2 E_x}{\partial x^2} \frac{n_x^2}{n_z^2} + \frac{\partial^2 E_x}{\partial y^2} + (k_o^2 n_x^2 - \beta_x^2) E_x = 0 \quad (4)$$

where β_x is the propagation constant of the E_{pq}^x mode. Solving (2) and (4) with proper boundary conditions becomes very tedious, and therefore we seek an approximate solution that is sufficiently accurate. We observe that, for most practical waveguide structures, the ratio n_x/n_z (or n_y/n_z) is almost constant in all regions. This enables us to use the method of separation of variables [7] to solve (2) and (4). Thus, we consider the actual waveguide as a perturbed form of the waveguide described by the following index distribution:

$$n_i^2(x, y) = n_i^2(x) + n_i^{\prime 2}(y) \quad (5)$$

where

$$n_i^2(x) = \begin{cases} \frac{n_{1i}^2}{2}, & |x| < \frac{a}{2} \\ n_{2i}^2 - \frac{n_{1i}^2}{2}, & |x| > \frac{a}{2} \end{cases} \quad (6)$$

$$n_i^{\prime 2}(y) = \begin{cases} n_{3i}^2 - n_{1i}^2/2, & y > b/2 \\ n_{1i}^2/2, & |y| < b/2 \\ n_{2i}^2 - n_{1i}^2/2, & y < -b/2 \end{cases}$$

and $i = x, y$ corresponds to E_{pq}^x, E_{pq}^y modes, respectively. The above profile matches with the actual profile in every region except in the corner (shaded) regions, where the two profiles differ by an amount $n_{1i}^2 - n_{2i}^2$, which is very small for most practical waveguides, and can be taken into account using first-order perturbation theory.

Using a procedure similar to that outlined in [7], we obtain

$$E_i = X_i(x) Y_i(y) \quad (7)$$

where

$$X_i(x) = \begin{cases} A \begin{pmatrix} \cos \kappa_i x \\ \sin \kappa_i x \end{pmatrix} & |x| < a/2 \\ B \exp(-\gamma_i |x|) & |x| > a/2 \end{cases} \quad (8)$$

$$Y_i(y) = \begin{cases} D \exp(-\delta_i y) & y > b/2 \\ C_1 \cos \alpha_i y + C_2 \sin \alpha_i y & |y| < b/2 \\ E \exp(\eta_i y) & y < -b/2 \end{cases}$$

and

$$\begin{aligned} \kappa_i &= a_1 \left(k_o^2 \frac{n_{1i}^2}{2} - \beta_{1i}^2 \right)^{1/2} \\ \gamma_i &= a_1 [\beta_{1i}^2 - k_o^2 (n_{2i}^2 - n_{1i}^2/2)]^{1/2} \\ \delta_i &= a_2 [\beta_{2i}^2 - k_o^2 (n_{3i}^2 - n_{1i}^2/2)]^{1/2} \\ \eta_i &= a_2 [\beta_{2i}^2 - k_o^2 (n_{2i}^2 - n_{1i}^2/2)]^{1/2} \\ a_i &= a_2 (k_o^2 n_{1i}^2/2 - \beta_{2i}^2)^{1/2}. \end{aligned} \quad (9)$$

A, B, C_1, C_2, D , and E are arbitrary constants, which finally results in only one independent amplitude constant in the expression for the field

$$\begin{cases} a_1 = n_{1z}/n_{1x}, a_2 = 1 & \text{for } i = x \\ a_1 = 1, a_2 = n_{1z}/n_{1y} & \text{for } i = y \end{cases} \quad (10)$$

The separation constants β_{1i} and β_{2i} are determined as solutions of transcendental equations obtained by applying proper boundary conditions, and the propagation constant of the mode is given by

$$\beta_i^2 = \beta_{1i}^2 + \beta_{2i}^2. \quad (11)$$

For E_{pq}^y modes, the boundary conditions under the assumption of polarized modes require that E_y and $\partial E_y/\partial x$ be continuous at $x = \pm a/2$ and $n_i^2 E_y, \partial E_y/\partial y$ be continuous at $y = \pm b/2$, which results in the following two transcendental equations:

$$\kappa_y a = 2 \tan^{-1}(\gamma_y/\kappa_y) + (p-1)\pi \quad (12)$$

$$\alpha_y b = \tan^{-1} \left(\frac{n_{1y}^2 \delta_y}{n_{3y}^2 \alpha_y} \right) + \tan^{-1} \left(\frac{n_{1y}^2 \eta_y}{n_{2y}^2 \alpha_y} \right) + (q-1)\pi, \quad p, q = 1, 2, 3, \dots \quad (13)$$

Similarly, for the E_{pq}^x modes, using the boundary condition of continuity of $E_x, \partial E_x/\partial y$ at $y = \pm b/2$ and $n_i^2 E_x, \partial E_x/\partial x$ at $x = \pm a/2$, we obtain

$$\kappa_x a = 2 \tan^{-1} \left(\frac{n_{1x}^2 \gamma_x}{n_{2x}^2 \kappa_x} \right) + (p-1)\pi \quad (14)$$

$$\alpha_x b = \tan^{-1} \left(\frac{\delta_x}{\alpha_x} \right) + \tan^{-1} \left(\frac{\eta_x}{\alpha_x} \right) + (q-1)\pi. \quad (15)$$

Using the first-order perturbation theory to account for the effect of corners [7], we obtain the corrected propagation constant β'_i as

$$\beta'_i{}^2 = \beta_i^2 + \Delta \beta_i^2 \quad (16)$$

where

$$\Delta \beta_i^2 = \frac{\frac{2k_o^2 t}{\gamma_i} \cos^2 \left(\kappa_i \frac{a}{2} \right) (n_{1i}^2 - n_{2i}^2) (sG_i + s'H_i)}{\left\{ \left[a + \frac{\sin \kappa_i a}{\kappa_i} + \frac{2t}{\gamma_i} \cos^2 \left(\kappa_i \frac{a}{2} \right) \right] \right.} \quad (17)$$

$$\left. \cdot x \left[(1 + F_i^2) b + \frac{\sin \alpha_i b}{\alpha_i} (1 - F_i^2) + sG_i + s'H_i \right] \right\}$$

and

$$F_i = \frac{(\eta_i/\alpha_i) \cos(\alpha_i b/2) - \sin(\alpha_i b/2)}{(\eta_i/\alpha_i) \sin(\alpha_i b/2) + \cos(\alpha_i b/2)}$$

$$G_i = \frac{[\cos(\alpha_i b/2) + F_i \sin(\alpha_i b/2)]^2}{\delta_i}$$

$$H_i = \frac{[\cos(\alpha_i b/2) - F_i \sin(\alpha_i b/2)]^2}{\eta_i}$$

$$t = n_{1i}^4/n_{2i}^4, s = s' = 1 \text{ for } E_{pq}^x \text{ modes } (i = x)$$

$$t = 1, s = n_{1i}^4/n_{3i}^4, s' = n_{1i}^4/n_{2i}^4 \text{ for } E_{pq}^y \text{ modes } (i = y). \quad (18)$$

III. RESULTS AND DISCUSSIONS

In order to test the accuracy of the present analysis, we have made calculations for a channel waveguide considered by Mabaya *et al.* [3], who have used the finite-element method which is expected to give highly accurate results. The channel waveguide is characterized by (see [3, fig. 3])

$$\begin{aligned} n_{1x} &= 2.222, n_{1y} = n_{1z} = 2.3129 \\ n_{2x} &= 2.20, n_{2y} = n_{2z} = 2.29 \\ n_3 &= 1.0, a = 5 \mu\text{m}, b = 1 \mu\text{m}. \end{aligned} \quad (19)$$

Fig. 2 shows the variation of β/k_o versus bk_o for the E_{11}^y , E_{21}^y , and E_{31}^y modes. Solid lines correspond to those of Mabaya *et al.* [3], while crosses and dashed lines correspond to our calculations [9]. We must mention here that the mode depicted as E_{21} in [3] should have been designated as E_{31} , since it seems to correspond to the second symmetric mode along the x -direction. We have confirmed this by comparing our results with those of Marcatili [8] for E_{11} , E_{21} , and E_{31} modes in isotropic waveguides. As can be seen from Fig. 2, the agreement between our results and those of the finite-element method is very good. The accuracy of the present method decreases for higher order modes due to increased field penetration into the corner regions; again, for the same reason, the results are expected to deviate by a small amount from the exact ones near cutoff. However, the agreement between the results of the present method and those of the finite-element method appears to be very good, even near cutoff for the fundamental mode. This can be attributed to the large a/b ratio of the waveguide under consideration, because, for large values of a/b , the waveguide effectively approaches the slab configuration for which this kind of analysis becomes exact. Further, the superstrate index (n_3) is much smaller than the core index, resulting in relatively stronger confinement even near cutoff, which is determined by the substrate index (n_2). For example, for the waveguide described by (19), we have found that the effect of the perturbation is almost negligible (less than 0.05 percent in β/k_o values). However, the effect of perturbation becomes significant for immersed structures ($n_3 = n_2$) and waveguides with smaller a/b ratios [7].

We have also compared the results obtained by our method with those of [5]. Fig. 3 shows the variation of normalized propagation constant B with k_o for E_{11}^x mode for a waveguide characterized by uniaxial substrate and channel with $n_o = 2.28$, $n_e = 2.17$ in the substrate and $n_o = 2.29$, $n_e = 2.21$ in the channel. The upper set corresponds to optic axis along x -direction and the lower set corresponds to optic axis along z -direction. Solid curves correspond to our unperturbed results and that of [5], while dashed curves correspond to our results with perturbation.

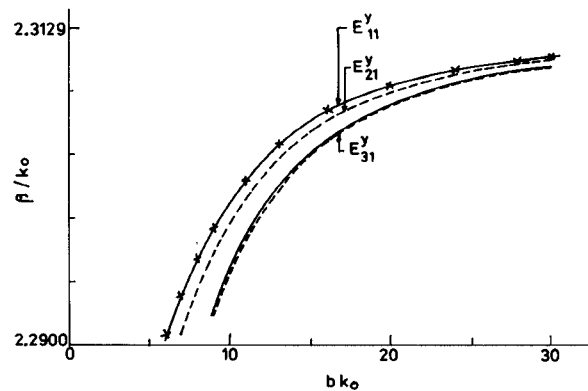


Fig. 2. Variation of β/k_o of E_{pq}^y modes with bk_o for an anisotropic channel waveguide described by (19). Solid lines correspond to the results of Mabaya *et al.* using the finite-element method. Crosses and dashed lines correspond to the present analysis.

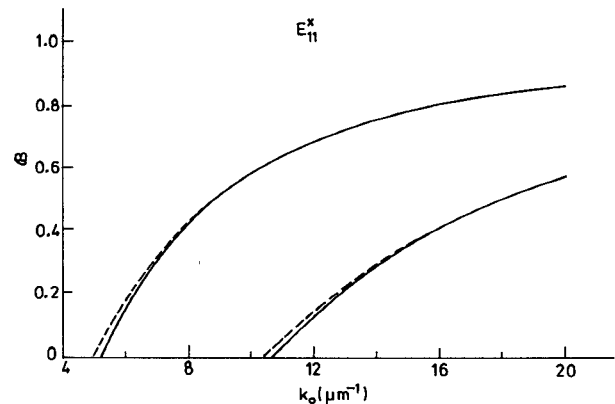


Fig. 3. Variation of normalized propagation constant B with k_o for E_{11}^x mode for a waveguide characterized by uniaxial substrate and channel with $n_o = 2.28$, $n_e = 2.17$ in the substrate and $n_o = 2.29$, $n_e = 2.21$ in the channel. The upper set corresponds to optic axis along x -direction and the lower set corresponds to optic axis along z -direction. Solid curves correspond to our unperturbed results and that of [5], while dashed curves correspond to our results with perturbation.

with k_o . Although [5] considers the variation of n_x/n_z and n_y/n_z in the various regions, the effect of corners is neglected. We have found that the effect of the former is within 0.001 percent, while the latter has a maximum effect of 0.1 percent (near cutoff) in β/k_o values (see Fig. 3). The former has much less effect because of the almost equal values of n_x/n_z and n_y/n_z in the substrate and channel regions, and due to the negligible field in the cover where again the above ratio differs only by about 3 percent. Therefore, it is more important to consider the effect of corners and one may neglect the nonconstancy of the ratio n_x/n_z or n_y/n_z in the various regions. Thus, the present method is more accurate and also involves only simple (uncoupled) transcendental equations which can be solved using a pocket calculator.

IV. CONCLUSION

We have presented an accurate and simple perturbation method to obtain the propagation characteristics of anisotropic rectangular core waveguides described by a diagonal dielectric constant tensor. The analysis should serve as a simple basis in the study of anisotropic channel waveguides, directional couplers, etc., and, in particular, may be applicable without modification to waveguides fabricated in LiNbO_3 using proton-diffusion technique [10].

$$B = \frac{\beta/k_o - n_{2i}}{n_{1i} - n_{2i}}$$

ACKNOWLEDGMENT

The authors wish to thank Professor A. K. Ghatak for his constant encouragement.

REFERENCES

- [1] See, for example, R. C. Alferness, "Guided wave devices for optical communication," *IEEE J. Quantum Electron.*, vol. QE-17, pp 946-959, June 1981.
- [2] P. Vandenbulcke and P. E. Lagasse, "Eigen mode analysis of anisotropic optical fibers or integrated optical waveguides," *Electron. Lett.*, vol. 12, pp 120-122, 1976.
- [3] N. Mabaya, P. E. Lagasse, and P. Vandenbulcke, "Finite element analysis of optical waveguides," *IEEE Trans. Microwave Theory Tech.*, vol. MTT-29, pp 600-605, June 1981.
- [4] M. Koshiba and M. Suzuki, "Finite element analysis of anisotropic optical waveguides," in *Proc. 4th Int. Conf. Integ. Opt. and Opt. Fiber Commun.*, Tokyo, Japan, 1983, paper 28D3.
- [5] R. A. Steinberg and T. G. Giallorenzi, "Modal fields of anisotropic channel waveguide," *J. Opt. Soc. Amer.*, vol. 67, pp 523-533, Apr. 1977.
- [6] G. B. Hocker and W. K. Burns, "Mode dispersion in diffused channel waveguides by the effective index method," *Appl. Optics*, vol. 36, pp 113-118, Jan. 1977; and M. N. Armenise and Marco De Sario, "Optical rectangular waveguide in titanium-diffused lithium niobate having its optical axis in the transverse plane," *J. Opt. Soc. Amer.*, vol. 72, pp 1514-1521, Nov. 1982.
- [7] A. Kumar, K. Thyagarajan, and A. K. Ghatak, "Analysis of rectangular-core dielectric waveguides: An accurate perturbation approach," *Opt. Lett.*, vol. 8, pp 63-65, Jan. 1983.
- [8] E. A. J. Marcatili, "Dielectric rectangular waveguide and directional coupler for integrated optics," *Bell Syst. Tech. J.*, vol. 48, pp 2071-2102, 1969.
- [9] The curves in [3, fig. 3] correspond to E_{pq}^y modes and not to E_{pq}^x modes as denoted in the figure, since β/k_0 values for E_{pq}^x modes will lie between 2.222 and 2.20, while that of E_{pq}^y modes will lie between 2.3129 and 2.29. This is also consistent with their earlier paper [2].
- [10] J. L. Jackel, C. E. Rice, and J. J. Veselka, "Proton exchange for high index waveguides in LiNbO_3 ," *Appl. Phys. Lett.*, vol. 41, pp 607-608, Oct. 1982.

The Interdigitated Three-Strip Coupler

S. M. PERLOW, SENIOR MEMBER, IEEE, AND A. PRESSER,
MEMBER, IEEE

Abstract — A general design procedure for three-strip interdigitated couplers with arbitrary coupling values is presented. These results are then applied, for various coupling values, to both stripline and microstrip media to check the physical realizability. The dimensions of the coupler can be substantially affected by allowing a small degree of impedance mismatching.

I. INTRODUCTION

Interdigitated three-line microstrip couplers have been described in the literature [1], [2]. Their dimensions were arrived at in a form which required rather complicated mathematical manipulations and optimization techniques. The approach taken here is to develop the capacitance matrix for the generalized three-line interdigitated coupler. Using this matrix, the parameters required to provide any degree of coupling in any type of media (inhomogeneous microstrip or homogeneous stripline) are easily derived.

Manuscript received January 25, 1984; revised May 16, 1984.

The authors are with RCA Laboratories, David Sarnoff Research Center, Princeton, NJ 08540.

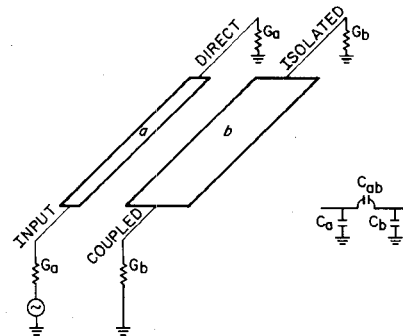


Fig. 1. Unequal width two-line coupler.

II. ASYMMETRICAL COUPLED LINES IN HOMOGENEOUS MEDIA

The construction of three-line couplers generally requires knowledge of the electrical characteristics of asymmetrical coupled lines. Cristal introduced the concept of unequal odd-mode and even-mode admittances for each individual line of a set of coupled lines of unequal widths in a homogeneous media [3]. The electrical characteristics of the coupled-line directional coupler are completely specified by either the capacitances per unit length or the odd and even mode admittances. The relationship between the coupler parameters, the coupling ratio and terminating admittances, and the line parameters as developed by Cristal are summarized in the following discussion.

Fig. 1 shows the coupler formed by line a and line b , both of which have an electrical length of ninety degrees. The odd and even mode admittances of each line are related to the per unit length mutual capacitance C_{ab} and the self capacitances C_a and C_b . These admittances are also related to the voltage coupling coefficient k and the respective terminating admittances G_a and G_b . The odd and even mode admittances can be expressed as

line a

$$Y_{oe}^{(a)} = vC_a = \frac{G_a - k\sqrt{G_a G_b}}{\sqrt{1 - k^2}} \quad (1)$$

$$Y_{oo}^{(a)} = 2vC_{ab} + vC_a = \frac{G_a + k\sqrt{G_a G_b}}{\sqrt{1 - k^2}} \quad (2)$$

line b

$$Y_{oe}^{(b)} = vC_b = \frac{G_b - k\sqrt{G_a G_b}}{\sqrt{1 - k^2}} \quad (3)$$

$$Y_{oo}^{(b)} = 2vC_{ab} + vC_b = \frac{G_b + k\sqrt{G_a G_b}}{\sqrt{1 - k^2}} \quad (4)$$

in which v is the velocity of propagation in the line media. Also note that $Y_{oo}^{(a)}$ is the odd-mode admittance of line a with respect to line b and $Y_{oo}^{(b)}$ is the odd-mode admittance of line b with respect to line a . If the width of each line in Fig. 1 were made equal, the coupler becomes symmetric with equal self capacitances C and equal terminating admittances G_o .

III. THE THREE-LINE COUPLER IN HOMOGENEOUS MEDIA

The general three-line coupler is formed by lines 1, 2, and 3 as shown in Fig. 2 together with the self and mutual capacitance representation. Lines 1 and 3 are tied on both ends to form a four-port coupler structure. For the same desired coupler perfor-